

# Pharmacologic inhibitors of I $\kappa$ B kinase suppress growth and migration of mammary carcinosarcoma cells *in vitro* and prevent osteolytic bone metastasis *in vivo*

Aymen I. Idris,<sup>1</sup> H el ene Libouban,<sup>2</sup>  
Herv e Nyangoga,<sup>2</sup> Euphemie Landao-Bassonga,<sup>1</sup>  
Daniel Chappard,<sup>2</sup> and Stuart H. Ralston<sup>1</sup>

<sup>1</sup>Bone Research Group, Institute of Genetic and Molecular Medicine, University of Edinburgh, General Western Hospital, Edinburgh, United Kingdom and <sup>2</sup>Institut National de la Sante et de la Recherche Medicale, U922, Facult e de M edecine, Angers, France

## Abstract

The NF- $\kappa$ B signaling pathway is known to play an important role in the regulation of osteoclastic bone resorption and cancer cell growth. Previous studies have shown that genetic inactivation of I $\kappa$ B kinase (IKK), a key component of NF- $\kappa$ B signaling, inhibits osteoclastogenesis, but the effects of pharmacologic IKK inhibitors on osteolytic bone metastasis are unknown. Here, we studied the effects of the IKK inhibitors celastrol, BMS-345541, parthenolide, and wedelolactone on the proliferation and migration of W256 cells *in vitro* and osteolytic bone destruction *in vivo*. All compounds tested inhibited the growth and induced apoptosis of W256 cells as evidenced by caspase-3 activation and nuclear morphology. Celastrol, BMS-345541, and parthenolide abolished IL1 $\beta$  and tumor necrosis factor  $\alpha$ -induced I $\kappa$ B phosphorylation and prevented nuclear translocation of NF- $\kappa$ B and DNA binding. Celastrol and parthenolide but not BMS-345541 prevented the activation of both IKK $\alpha$  and IKK $\beta$ , and celastrol inhibited IKK $\alpha$ / $\beta$  activation by preventing the phosphorylation of TAK1, a key receptor-associated factor upstream of IKK. Celastrol and parthenolide markedly reduced the mRNA expression of matrix metalloproteinase 9 and urinary plasminogen activator, and inhibited W256 migra-

tion. Administration of celastrol or parthenolide at a dose of 1 mg/kg/day suppressed trabecular bone loss and reduced the number and size of osteolytic bone lesions following W256 injection in rats. Histo-morphometric analysis showed that both compounds decreased osteoclast number and inhibited bone resorption. In conclusion, pharmacologic inhibitors of IKK are effective in preventing osteolytic bone metastasis in this model and might represent a promising class of agents to the prevention and treatment of metastatic bone disease associated with breast cancer. [Mol Cancer Ther 2009;8(8):2339-47]

## Introduction

Bone metastases are a common cause of morbidity in cancer patients and occur in up to 50% of patients of breast cancer, lung cancer, and prostate cancer (1-3). The major clinical manifestations of metastases are bone pain, pathologic fractures, and spinal cord compression (1, 2). Most bone metastases are osteolytic and are caused by release of factors by the invading tumor, which cause osteoclast activation and bone resorption (1, 4, 5). Inhibitors of bone resorption such as bisphosphonates have been shown to significantly reduce skeletal complications in patients with breast cancer, myeloma, and other tumor types but they are incompletely effective, indicating the need to identify new strategies for the prevention and treatment of patients with bone metastases (2). The NF- $\kappa$ B signaling pathway is known to play a role in both osteoclast activation and tumor cell growth (6). Ligand-induced activation of a number of cytokines and growth factor receptors including receptor activator of NF- $\kappa$ B (RANK), tumor necrosis factor (TNF) receptors, the interleukin 1 receptor, and the transforming growth factor  $\beta$  (TGF $\beta$ ) receptor result in recruitment of receptor associated factors including TGF $\beta$ -activated kinase 1 (TAK1) to the intracellular domain of the receptor (7). This triggers the phosphorylation and binding of the two catalytic subunits of the I $\kappa$ B kinase (IKK) complex, IKK $\alpha$ , and IKK $\beta$  to the regulatory subunit IKK $\gamma$  (7). Once activated, the IKK complex phosphorylates I $\kappa$ B and leads to nuclear translocation of a number of transcription factors including NF- $\kappa$ B and activator protein 1 (8). Over recent years, there has been increasing interest in the role of IKK in the regulation of tumorigenesis, metastases, and osteoclastic bone resorption (9). For example, genetic inactivation of IKK $\alpha$  or IKK $\beta$  results in a complete ablation of osteoclastogenesis and prevents inflammation-induced bone loss (10, 11), and in preliminary studies, we have found that pharmacologic inhibitors of IKK inhibit osteoclast formation *in vitro* and prevent ovariectomy induced bone loss *in vivo* (12). Furthermore, IKK activation is also known to promote the proliferation of

Received 2/13/09; revised 5/22/09; accepted 5/22/09; published OnlineFirst 8/11/09.

**Grant support:** A.I. Idris is supported by the European Calcified Tissue Society/AMGEN fellowship. A.I. Idris is partly supported by a grant from the Arthritis Research Campaign and is a receipt of European Calcified Tissue Society/AMGEN fellowship.

The costs of publication of this article were defrayed in part by the payment of page charges. This article must therefore be hereby marked *advertisement* in accordance with 18 U.S.C. Section 1734 solely to indicate this fact.

**Note:** Supplementary material for this article is available at Molecular Cancer Therapeutics Online (<http://mct.aacrjournals.org/>).

**Requests for reprints:** Aymen I. Idris, Bone Research Group, Institute of Genetic and Molecular Medicine, University of Edinburgh, General Western Hospital, Edinburgh, EH4 2XU. Phone: 0131-651-1032; Fax: 0131-651-1085. E-mail: aymen.idris@ed.ac.uk

Copyright   2009 American Association for Cancer Research.

doi:10.1158/1535-7163.MCT-09-0133

cancer cells, and small molecule inhibitors of IKK have been shown to prevent the development of distant metastases in a number of disease models (13–19). In view of this, pharmacologic inhibitors of IKK $\alpha$  and IKK $\beta$  might be expected to be of particular value in the prevention of osteolytic disease, but the effects of IKK inhibitors on bone metastases have not been previously investigated. Here, we investigated the effects of these inhibitors in a well-established model of metastatic bone disease associated with breast cancer induced by intracardiac injection of W256 mammary carcinoma cells (20, 21).

## Materials and Methods

### Drugs and Reagents

Celastrol, parthenolide, BMS-345541, and wedelolactone were purchased from CalBiochem. All chemicals were obtained from Sigma (Dorset), unless otherwise indicated. All culture media were obtained from Invitrogen. Human IL-1 $\beta$  was obtained from Roche (London) and human macrophage colony stimulating factor, human TNF $\alpha$ , TGF $\beta$ , and bone morphogenic protein 2 were obtained from R&D Systems. 1,25 (OH) $_2$ -vitamin D $_3$  was obtained from Alexis Biochemicals. Rat Swiss Walker 256 cells (W256) were a gift from Professor Daniel Chappard (Institut National de la Sante et de la Recherche Medicale, Angers, France).

### Measurement of W256 Viability

Rat W256 cells were maintained in DMEM supplemented with 10% FCS and penicillin at 37°C in 5% CO $_2$ . Before experimentation, the cells were seeded into 96-well plates at  $5 \times 10^3$  cells per well or 48-well plates at  $12 \times 10^3$  cells per well in culture medium and left to adhere overnight. Cell number was determined by adding 10% (v/v) of Alamar Blue reagent to each well. The cells were incubated for a further 3 h and fluorescence measured (excitation, 530 nm; emission 590 nm) using a Biotek Synergy HT plate reader.

### Morphologic Assessment of Apoptosis

Rat W256 cells were seeded in 48-well plates at  $12 \times 10^3$  cells per well, or 12-well plates at  $200 \times 10^3$  cells per well in culture medium. Following treatments, both adherent and nonadherent cells were collected and cytospun onto glass slides. Apoptosis was detected by the characteristic changes in nuclear morphology following 4,6-diamidino-2-phenylindole staining as previously described in Idris et al. (22). Cells with clearly fragmented DNA were counted and expressed as a percentage of total cell number.

### Assessment of W256 Migration

W256 cells were seeded into 48-well plates ( $500 \times 10^3$  cells per well) and allowed to grow to confluence over a period of 48 h. W256 migration was assessed using the wound healing assay as previously described in Serrels et al. (23). Briefly, confluent monolayers of W256 were scored with a fine pipette tip to produce a gap in the cell layer and then the cells were treated with either vehicle or test compounds for 16 h. Migration of W256 cells into the gap was monitored and visualized by phase-contrast light microscopy.

### Western Blotting

W256 cells were seeded in 12-well plates to confluence and treated with test compounds for the desired period of time. Following the incubation period, the drug/vehicle-containing medium was removed and the monolayer was rinsed with ice-cold PBS. Adherent cells were then gently scraped in standard lysis buffer [0.1% (w/v) SDS, 0.5% (w/v) sodium deoxycholate, 1% Triton X-100, 1 mmol/L EDTA, and 2% (v/v) protease inhibitor cocktail (Sigma)]. For studies involving extraction of phosphorylated proteins, 10 mmol/L of sodium fluoride and 2% (v/v) phosphatase inhibitor cocktail (Sigma) were added to the standard lysis buffer described above. For studies involving immunoprecipitation of proteins, 10 mmol/L of sodium fluoride and 2% (v/v) phosphatase inhibitor cocktail (Sigma) and sodium orthovanadate (1 mmol/L) were added to the standard lysis buffer described above. The lysate was incubated on ice for 10 min and spun at 12,000 *g* at 4°C for 10 min. The supernatant was collected and the protein concentration was determined using BCA assay (Pierce). Total protein (30–50  $\mu$ g) was resolved by SDS-PAGE on 4% to 12% polyacrylamide SDS gels, transferred onto polyvinylidene difluoride membranes (BioRAD), and immunoblotted with antibodies according to manufacturer's instructions. Activated (cleaved, p-19) caspase-3 and phosphorylated TAK1 levels were detected using a goat polyclonal anti-caspase-3 antibody and anti-p-TAK1 (Santa Cruz Biotechnology). Detection of native and phosphorylated I $\kappa$ B, IKK $\alpha/\beta$ , and IKK $\beta$  was done using rabbit monoclonal antibodies (Cell Signaling Technology). The immunocomplexes were visualized by an enhanced chemiluminescence detection kit (Pierce) by using horseradish peroxidase-conjugated secondary antibody.

### Detection of NF- $\kappa$ B Activation

Immunostaining for p65 NF- $\kappa$ B was done essentially as previously described in Idris et al. (24). Briefly, W256 cells were fixed in 4% formaldehyde and permeabilised in 0.1% Triton X100 for 10 min. Cells were stained with rabbit anti-NF- $\kappa$ B p65 (Santa) and Alexa Fluor 488-conjugated goat-anti-Rabbit secondary antibody (Invitrogen) and then visualized using a Zeiss fluorescence microscope.

### Measurement of p65 NF- $\kappa$ B DNA Binding

W256 cells were seeded in 12-well plates to confluence and treated with test compounds for the desired period of time. Following the incubation period, nuclear extracts were prepared using a nuclear extract kit (Active Motif) and nuclear translocation was measured using TRANSAM ELISA kits for p65 NF- $\kappa$ B (Active Motif) according to the manufacturers instructions.

### Quantitative PCR

Quantitative PCR was used to detect gene expression in osteoblast and W256 cells. Briefly, cells were lysed using TRIzol reagent, separated with chloroform and precipitated with isopropyl alcohol. The pellet was washed with 70% ethanol, and suspended in DEPC-treated water. RNA was quantified using a RiboGreen dye kit (Invitrogen) according to manufacturer's instructions. Complementary DNA

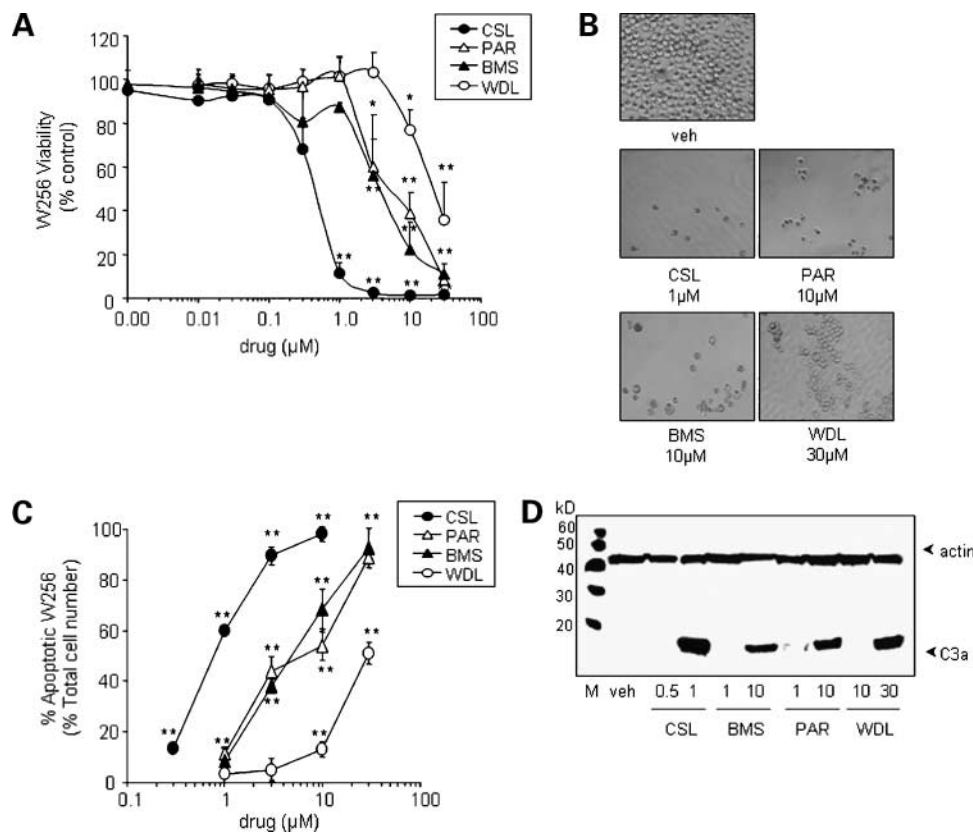


**Figure 1.** IKK inhibitors suppress viability, induce caspase-3 activation, and cause apoptosis in W256 *in vitro*. The mammary carcinosarcoma Swiss Walker cells (W256) were treated with vehicle (*veh*; 0.1% DMSO) or test agent indicated at 0.1 to 30  $\mu\text{mol/L}$  for 24 h (D) or 48 h (A, B, and C). A, W256 numbers were determined by AlamarBlue assay and expressed as a percentage of the values found in control cultures. B, representative photomicrographs of W256 exposed to vehicle (0.1% DMSO), or celestrol, parthenolide, BMS-345541, or wedelolactone at indicated concentration. C, apoptotic cells were visualized by 4,6-diamidino-2-phenylindole staining and cells with fragmented DNA were counted and expressed as a percentage of the total cell number. Points, means obtained from three independent experiments; bars, SD.  $P < 0.01$  (\*\*) or  $P < 0.05$  (\*) from vehicle treated. D, Western blot analysis done in W256 treated with vehicle (0.1% DMSO) or indicated compound for 24 h. Total cellular protein was subjected to Western blot analysis (50  $\mu\text{g}$  per lane) using active caspase 3 (C3a) or antiactin antibodies. The results shown are representative of three independent experiments. M, marker; p, phosphorylated; CSL, celestrol; PAR, parthenolide; BMS, BMS-345541; WDL, wedelolactone.

was generated from quantified RNA using Invitrogen SuperScript III Reverse Transcriptase kit according to manufacturer's instructions. The product was cleaned using a PCR purification kit (Invitrogen) according to manufacturer's instructions, and then run and visualized on a 1.5% agarose gel (SYBR green dye) adjacent to a low-molecular-weight ladder. Primers were designed using the Ensembl genome browser and Roche Web site. Primers used are as follows: matrix metalloproteinase 9 (MMP9)—forward (gatctgtaccgcaggcactc), reverse (aagttctctccacggctctt); parathyroid hormone related protein (PTHrP)—forward (cactactgtaaatg-cattgggatca), reverse (tggattagccttggcaaaaa); urinary plasminogen activator (uPAR)—forward (caggacctctgcagaacca), reverse (gcacaggcctctgtgtcac); vascular endothelial growth factor—forward (aaaaacgaaagcgcaagaaa), reverse (tttctccgctctgaacaagg). Levels of gene expression were calculated as copy number per microgram of total RNA and expressed as percentage of control.

#### Animals and Osteolytic Bone Destruction *In vivo*

We investigated the effects of IKK inhibitors on osteolytic bone metastases using the rat W256 model of osteolytic bone metastases as described in Blouin et al. (20). Briefly, 36 male Wistar rats received intracardiac injection of W256 tumor cells ( $10^7$  cells) followed by i.p. injection of either celestrol (1 mg/kg/d) or parthenolide (1 mg/kg/d) in vehicle containing DMSO/Cremaphor/PBS (1:1:8). Dosages and treatment regimes used for parthenolide and celestrol were chosen based on previous *in vivo* studies that showed that these agents have both anti-inflammatory and antitumor effects (18, 25–28). Controls received vehicle. Animals were sacrificed 10 d after injection and both tibias and femurs were analyzed by radiography and microCT using a Skyscan 1172 scanner (29). To study the effects on tumor growth within bone, whole tibial metastases area was measured on two-dimensional microCT images using image J software (release 1.34s-NIH-USA) and results were expressed as a

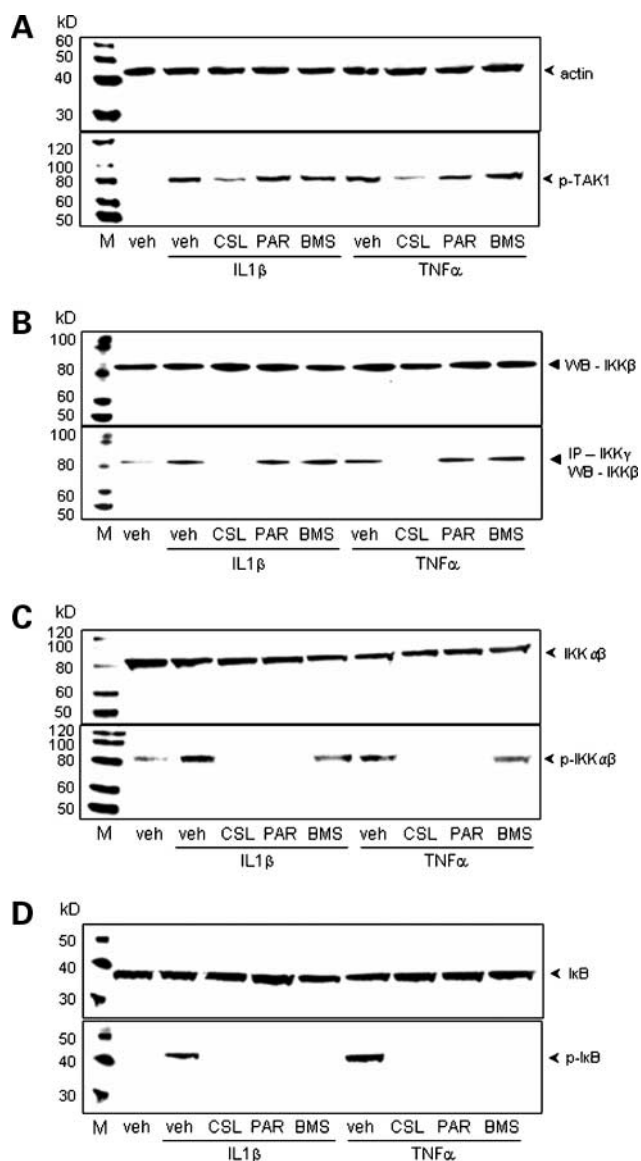


**Figure 2.** The IKK inhibitors celastrol (CSL) and parthenolide (PAR) abolish IL1 $\beta$  and TNF $\alpha$ -induced IKK activation in W256 *in vitro*. The mammary carcinosarcoma cells W256 were treated with vehicle (veh; 0.1% DMSO) or celastrol (1  $\mu$ mol/L), parthenolide (PAR; 20  $\mu$ mol/L), and BMS-345541 (BMS; 20  $\mu$ mol/L) for 1 h before stimulation with IL1 $\beta$  (8  $\mu$ g/mL) or TNF $\alpha$  (100 ng/mL) for 2 min (A–C) or 5 min (D). **A**, **C**, and **D**, total cellular protein was subjected to Western blot analysis (50  $\mu$ g per lane) using phosphorylated TAK1 (p-TAK1), IKK $\alpha/\beta$  (p-IKK $\alpha/\beta$ ), phosphorylated I $\kappa$ B (p-I $\kappa$ B), I $\kappa$ B, or antiactin antibodies. **C**, cellular protein was subjected to immunoprecipitation using IKK $\gamma$  antibodies followed by Western blot analysis (50  $\mu$ g per lane) using IKK $\beta$  antibodies. The results shown are representative of three independent experiments. M, marker.

percentage of total metaphyseal area. Following scanning, the limbs were embedded and processed for bone histomorphometry as described (30, 31).

#### Statistical Analysis

Comparison between groups was by ANOVA followed by Dunnet's posttest using SPSS for Windows version 11. A *P* value of 0.05 or below was considered statistically sig-

nificant. The concentration that produced 50% of response (IC<sub>50</sub>) was calculated using GraphPad Prism 4 for Windows.

## Results

### IKK Inhibitors Induce Apoptosis of W256 Cells *In vitro*

To examine the effects of IKK inhibition on W256 proliferation and survival, we used celastrol, BMS-345541, parthenolide, and wedelolactone, which are commercially available compounds that have been shown to inhibit IKK activity (32–35). All four compounds tested inhibited W256 viability in a concentration-dependent manner over the concentration range 0.01 to 30  $\mu$ mol/L (Fig. 1A). The concentration at which the compounds inhibited W256 growth by 50% (IC<sub>50</sub>) was  $0.43 \pm 0.1$   $\mu$ mol/L for celastrol,  $4.7 \pm 2.1$   $\mu$ mol/L for BMS-345541,  $6.5 \pm 1$   $\mu$ mol/L for parthenolide, and  $26.9 \pm 7$   $\mu$ mol/L for wedelolactone. Exposure of W256 cultures to celastrol (1  $\mu$ mol/L), parthenolide (10  $\mu$ mol/L), BMS-345541 (10  $\mu$ mol/L), or wedelolactone (30  $\mu$ mol/L) caused the activation of caspase-3 within 16 hours, indicative of apoptosis (Fig. 1D). As shown in Fig. 1C, all compounds tested induced W256 apoptosis in a dose-dependant manner after 48 hours as evidenced by nuclear morphology (IC<sub>50</sub>,  $0.97 \pm 0.01$   $\mu$ mol/L for celastrol; IC<sub>50</sub>,  $6.5 \pm 0.7$   $\mu$ mol/L for parthenolide; and IC<sub>50</sub>,  $51.1 \pm 4$   $\mu$ mol/L for wedelolactone). The order of potency in inhibiting proliferation, stimulating caspase-3 activation, and inducing apoptosis in W256 was celastrol > parthenolide  $\geq$  BMS-345541 > wedelolactone.

### Celastrol and Parthenolide Prevent IKK $\alpha$ and IKK $\beta$ Activation in W256 *In vitro*

To gain an insight into the mechanism by which these compounds induce W256 apoptosis, we examined the activation of TAK1, IKK $\alpha/\beta$ , and I $\kappa$ B in the presence and absence of celastrol, BMS-345541, or parthenolide, which were the three most potent inhibitors of W256 cell growth. Treatment with IL1 $\beta$  (8  $\mu$ g/mL) or TNF $\alpha$  (100 ng/mL) caused phosphorylation of TAK1 and IKK $\alpha/\beta$  and the recruitment of IKK $\beta$  to the regulatory unit IKK $\gamma$  within 2 minutes, followed by I $\kappa$ B phosphorylation after 5 minutes (Fig. 2). Pretreatment of W256 with celastrol, BMS-345541, or parthenolide (0.1–20  $\mu$ mol/L) before stimulation with IL1 $\beta$  or TNF $\alpha$  inhibited phosphorylation of I $\kappa$ B in a dose-dependant manner (IC<sub>50</sub>,  $0.1 \pm 0.02$   $\mu$ mol/L for celastrol; IC<sub>50</sub>,  $12.1 \pm 1.3$   $\mu$ mol/L for BMS-345541; and IC<sub>50</sub>,  $14.6 \pm 2$   $\mu$ mol/L for parthenolide), with complete inhibition of I $\kappa$ B activity observed at concentrations of 1  $\mu$ mol/L for celastrol and 20  $\mu$ mol/L for parthenolide and BMS-345541 (Fig. 2D). This rank order of potency in W256 cells (celastrol > parthenolide = BMS) correlates with the efficacy of the three compounds in inhibiting cell growth and induction of apoptosis (Fig. 1). Celastrol inhibited the phosphorylation of TAK1 (Fig. 2A) and abolished binding of IKK $\beta$  to IKK $\gamma$  (Fig. 2B), whereas BMS-345541 and parthenolide showed no effects on both parameters. As shown in Fig. 2C, celastrol and parthenolide but not BMS-345541 inhibited IL1 $\beta$  and TNF $\alpha$  induced activation of IKK $\alpha$  and IKK $\beta$ , indicating a

strong inhibitory effect on both catalytic units of the IKK complex.

### Celastrol and Parthenolide Inhibit NF- $\kappa$ B Activation in W256 Cells *In vitro*

Because all components of the IKK complex are thought to play a key role on tumorigenesis (13–15, 36), we examined the effects of the IKK $\alpha$  and IKK $\beta$  Inhibitors celastrol and parthenolide on NF- $\kappa$ B activation in W256 cells. Preincubation of W256 with celastrol (1  $\mu$ mol/L) or parthenolide (20  $\mu$ mol/L) for 1 hour before stimulation with IL1 $\beta$  and TNF $\alpha$  caused a significant inhibition of NF- $\kappa$ B nuclear translocation (Fig. 3A) and DNA binding (Fig. 3B and C). None of the compounds tested affected TGF $\beta$  or bone morphogenic protein 2-induced Smad activation in W256 cells at concentrations that inhibited NF- $\kappa$ B activation and migration (Supplementary Fig. S1).

### Celastrol and Parthenolide Inhibit Migration of W256 Cells *In vitro*

We next studied the effects of celastrol and parthenolide on migration of W256 cells. Celastrol completely abolished the migration of the W256 at a concentration of 0.5  $\mu$ mol/L, within 16 hours of exposure, whereas the IKK $\alpha$ / $\beta$  inhibitor parthenolide (5  $\mu$ mol/L) was partially active (Fig. 4A). None of the compounds tested inhibited W256 viability (Fig. 4B) or induced caspase-3 activation (Fig. 4C) at this time point, indicating that the observed effects on cell migration was not mediated by an inhibitory effect on cell growth.

### IKK $\alpha$ / $\beta$ Inhibition Down-Regulate uPAR and MMP9 mRNA Expression in W256 *In vitro*

To investigate the mechanism by which IKK inhibitors suppress W256 migration, we studied the effects on mRNA

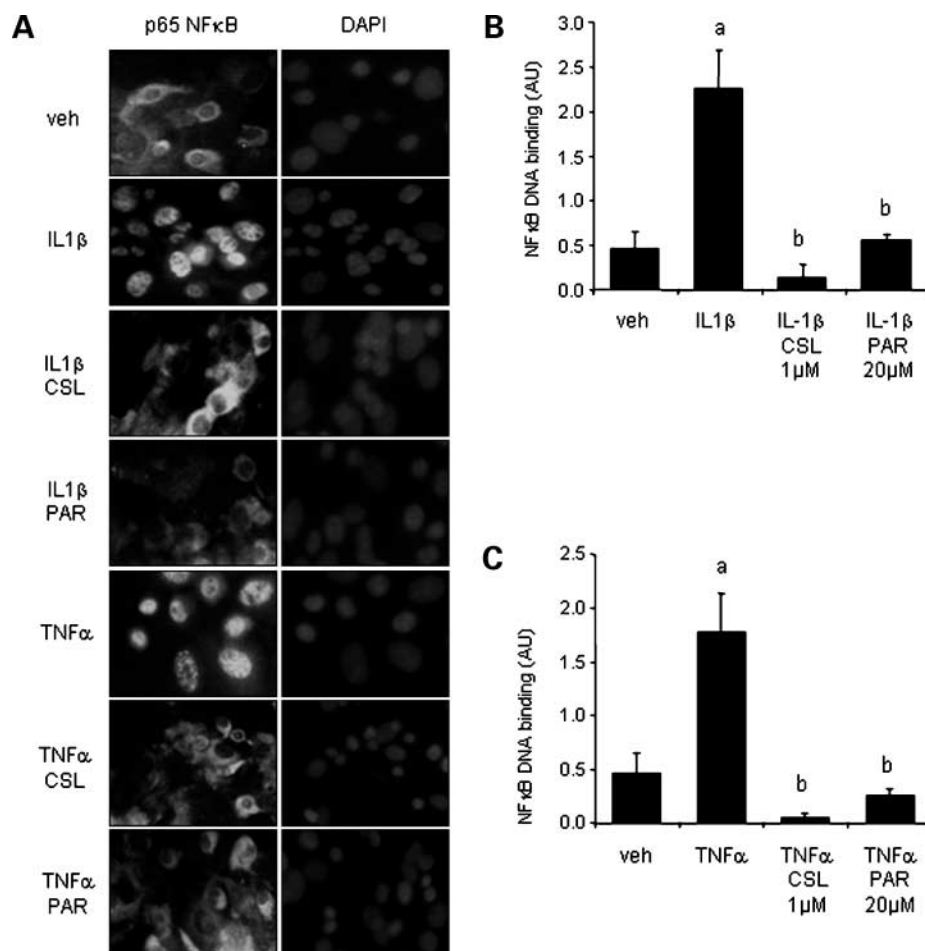


**Figure 3.** The IKK inhibitors celastrol (CSL) and parthenolide (PAR) abolish IL1 $\beta$ - and TNF $\alpha$ -induced NF- $\kappa$ B nuclear translocation in W256 *in vitro*. The mammary carcinosarcoma cells W256 were treated with vehicle (veh; 0.1% DMSO) or test agent at indicated concentration for 1 h and then stimulated with IL1 $\beta$  (8  $\mu$ g/mL) or TNF $\alpha$  (100 ng/mL) for 30 min. **A**, immunofluorescence microphotograph of W256 cells treated as described and stained for p65 NF- $\kappa$ B and 4,6-diamidino-2-phenylindole. **B** and **C**, nuclear extracts prepared and NF- $\kappa$ B DNA-binding activity analyzed using a TRANSAM ELISA. Columns, mean of three independent experiments, each done in duplicate; bars, SD. a,  $P < 0.05$  from vehicle; b,  $P < 0.05$  from cytokine stimulated.

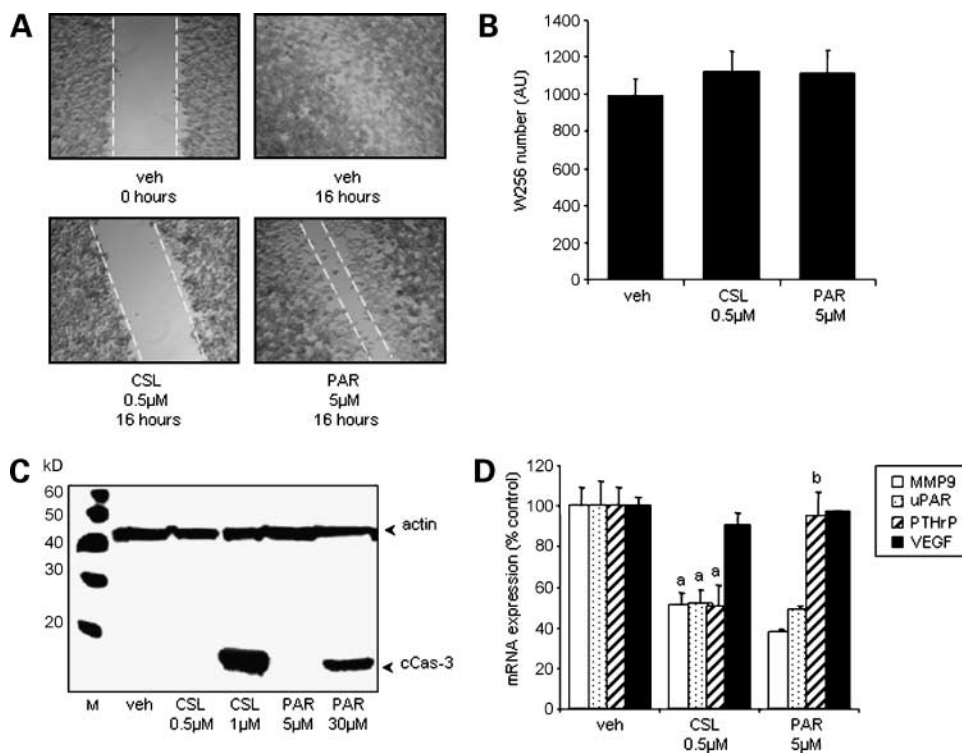


**Figure 4.** The IKK inhibitors celastrol (CSL) and parthenolide (PAR) inhibit the migration of W256 mammary carcinosarcoma cells without affecting cell viability *in vitro*. The mammary carcinosarcoma cells W256 were treated with vehicle (veh; 0.1% DMSO), celastrol (0.5 μmol/L), and parthenolide (5 μmol/L) for 16 h. W256 migration was assessed by wound healing assay (A) and cell viability, which was assessed by AlamarBlue assay (B). Western blot analysis for cleaved caspase-3 and actin in W256 cells exposed to the indicated compound for 16 h (C). D, mRNA expression of uPAR, PTHrP, MMP9, and vascular endothelial growth factor in W256 as measured by rt-PCR followed by quantitative PCR. Columns, means of three independent experiments; bars, SD. a,  $P < 0.05$  from vehicle; b,  $P < 0.05$  from CSL treated group.

expression of a number of genes that have been implicated in the regulation of cell migration using quantitative PCR. As shown in Fig. 4D, celastrol (0.5 μmol/L) and parthenolide (5 μmol/L) inhibited the mRNA expression of uPAR and MMP9 within 16 hours at concentrations inhibitory toward W256 migration. Celastrol (0.5 μmol/L) but not parthenolide (5 μmol/L) inhibited mRNA expression of PTHrP (Fig. 4D). Neither celastrol (0.5 μmol/L) nor parthenolide (5 μmol/L) inhibited mRNA expression of vascular endothelial growth factor in W256 cells (Fig. 4D).

#### Celastrol and Parthenolide Inhibit the Development of Osteolytic Metastases *In vivo*

We next investigated the effects of celastrol and parthenolide on osteolytic bone metastases *in vivo* using the W256 breast cancer cell model. All nine rats that were treated with vehicle developed significant trabecular bone loss below the growth plate visualized by X-ray indicative of osteolytic bone lesions, whereas this was significantly inhibited by treatment with celastrol (metastases developed in 1 of 9 animals;  $P < 0.01$ ) and by parthenolide (metastases developed in 2 of 11 animals;  $P < 0.01$ ). Further analysis by microCT showed that both celastrol (1 mg/kg/day) and parthenolide (1 mg/kg/day) significantly reduced the size of osteolytic lesions by up to 75% (Fig. 5A). Detailed microCT analysis of tumor size showed that both compounds at a daily dose of 1 mg/kg greatly reduced tumor size within osteolytic lesions in the metaphysis of the proximal tibia (Fig. 5A). Both compounds tested were also effective in preventing trabecular bone loss (Fig. 5C) and the increase in trabecular separation at the proximal tibia

(Fig. 5D). A detailed bone histomorphometric analysis showed that celastrol and parthenolide reduced osteoclast numbers (Fig. 6A and B), eroded surface (Fig. 6C) and the number of mononucleated TRAcP-positive cells within the bone marrow cavity (Fig. 6D).

#### Discussion

The NF-κB signaling pathway plays a key role in osteoclast activation and is also known to promote the proliferation of cancer cells and development of distant metastases. The IKK complex is critical for NF-κB activation by phosphorylating IκB, which is ubiquitinated and degraded by the proteasome, thereby releasing the p65 subunit of NF-κB, which translocates to the nucleus and activates gene transcription (7). Over recent years, interest has focused on the role of IKK as a therapeutic target for the treatment of tumor cell growth and osteoclastic bone resorption. Genetic inactivation of IKKβ inhibits osteoclastogenesis (11) and other studies have shown that pharmacologic and genetic inactivation of IKKα and IKKβ inhibit proliferation of cancer cells *in vitro* and prevent development of distant metastases *in vivo* (16, 17, 37). Taken together, these data suggest that IKK inhibitors might be particularly valuable in the treatment of cancers that metastasize to bone, but the effects of pharmacologic inhibitors of IKK on osteolytic bone loss are unknown.

Here, we studied the effects of four commercially available agents that have previously been reported to inhibit IKK activity (12, 26, 35, 38) on proliferation and migration

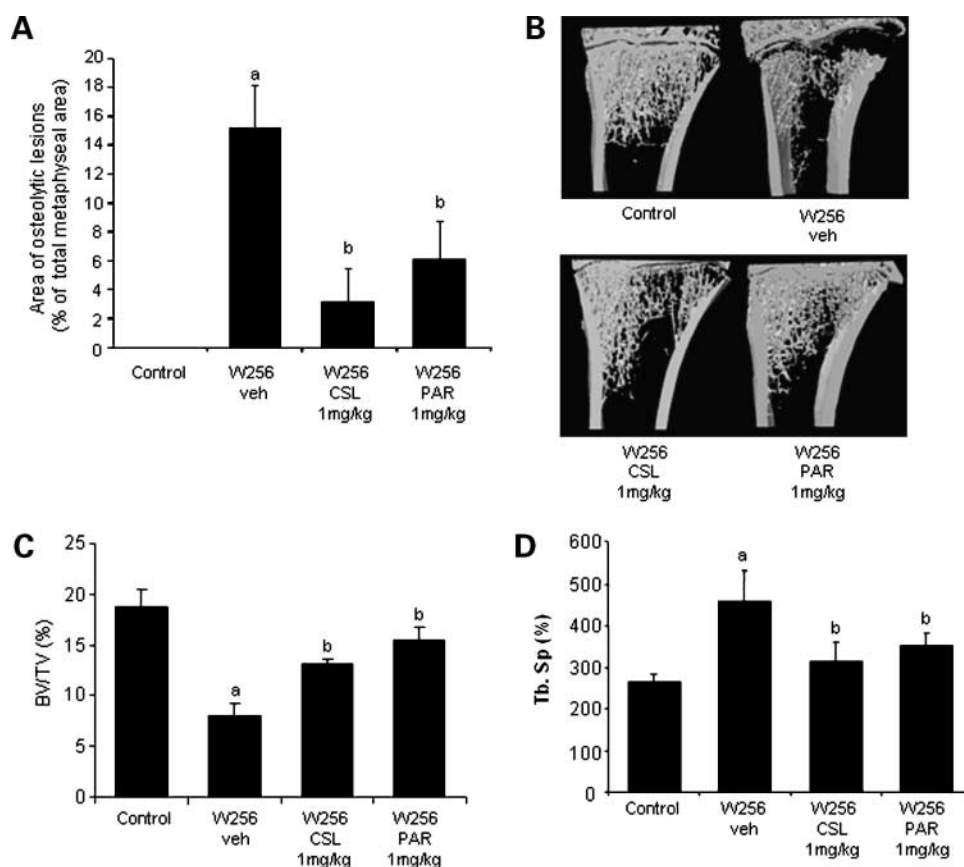
of W256 cells *in vitro* and osteolytic bone metastasis *in vivo*. Celestrol, parthenolide, BMS-345541, and wedelolactone inhibited the proliferation and induced apoptosis of W256 cells *in vitro*. There was a striking difference in potency between the compounds tested. Although parthenolide and BMS-345541 were equally potent, celestrol was significantly more active and induced W256 apoptosis at concentrations in the nanomolar range. Wedelolactone, on the other hand, was only active at concentrations >20  $\mu\text{mol/L}$ . This order of potency is in broad agreement with the previously reported efficacy of the four compounds at inhibiting IKK (12, 26, 35, 38) and suggests that they exert their antiproliferative and apoptotic effects by suppressing IKK activity. To investigate this hypothesis further, we conducted a number of experiments to examine activation of key components of the NF- $\kappa\text{B}$  pathway in W256 cells. Celestrol, parthenolide, BMS-345541, and wedelolactone all prevented phosphorylation of I $\kappa\text{B}$ , a key signaling protein down stream of IKK with an order of potency of celestrol > parthenolide = BMS-345541 > wedelolactone, similar to their effects on W256 proliferation and apoptosis, therefore suggesting an IKK-dependent effect. Further studies revealed that only celestrol and parthenolide inhibited activation of the two key catalytic component of the IKK complex, IKK $\alpha$  and IKK $\beta$ . Celestrol also prevented the binding of IKK $\beta$  to the regulatory unit IKK $\gamma$  of the IKK complex, whereas parthenolide

had no effect. This indicates that celestrol and parthenolide suppress the activation of the catalytic units of the IKK complex IKK $\alpha$  and IKK $\beta$  by distinct mechanisms. In support of this, we found that celestrol suppressed phosphorylation of TAK1, one of the key receptor recruitment factors upstream of the IKK complex. These findings are in agreement with recent reports that show that celestrol inhibits the recruitment of TAK1 to the intracellular domain of RANK and TNF receptors (12, 32).

Celestrol and parthenolide both inhibited migration of W256 cells after 16 hours without affecting cell number or apoptosis, but celestrol was much more potent. With longer exposure, however, both agents reduced cell number and stimulated apoptosis. These observations support the results of previous studies that have shown that IKK plays a key role in the regulation of cancer cell migration and the development of metastases (6, 17, 37). The greater potency of celestrol coupled with the fact that it inhibited expression of several genes that promote the development of metastases including PTHrP, MMP9, and uPAR suggests that signaling pathways downstream of TAK1 and/or independent of IKK activation may be responsible for the effects that we observed.

In addition to the *in vitro* effects observed, we also showed that celestrol and parthenolide at doses of 1 mg/kg/day inhibited the development of osteolytic lesions induced by

**Figure 5.** The IKK inhibitors celestrol (CSL) and parthenolide (PAR) prevent osteolytic bone destruction *in vivo*. Male Wistar rats at age of 16 wk received intracardiac injection of W256 tumor cells ( $10^7$  cells) followed by i.p. injection of either vehicle ( $n = 12$ ), celestrol (1 mg/kg/d;  $n = 12$ ), or parthenolide (1 mg/kg/d;  $n = 12$ ). Animals were sacrificed 10 d after injection and both tibias and femurs were visualised and analyzed by microCT. **A**, total area of osteolytic lesions expressed as a percentage of total metaphyseal area. **B**, representative microCT images from the tibial metaphysis. **C**, trabecular bone volume (BV/TV) from the same experiment as assessed by histomorphometric analysis. **D**, trabecular separation (Tb.Sp) as assessed by microCT analysis. Columns, means from 12 rats per group; bars, SEM. *a*,  $P < 0.05$  from vehicle; *b*,  $P < 0.05$  from W256-injected group.



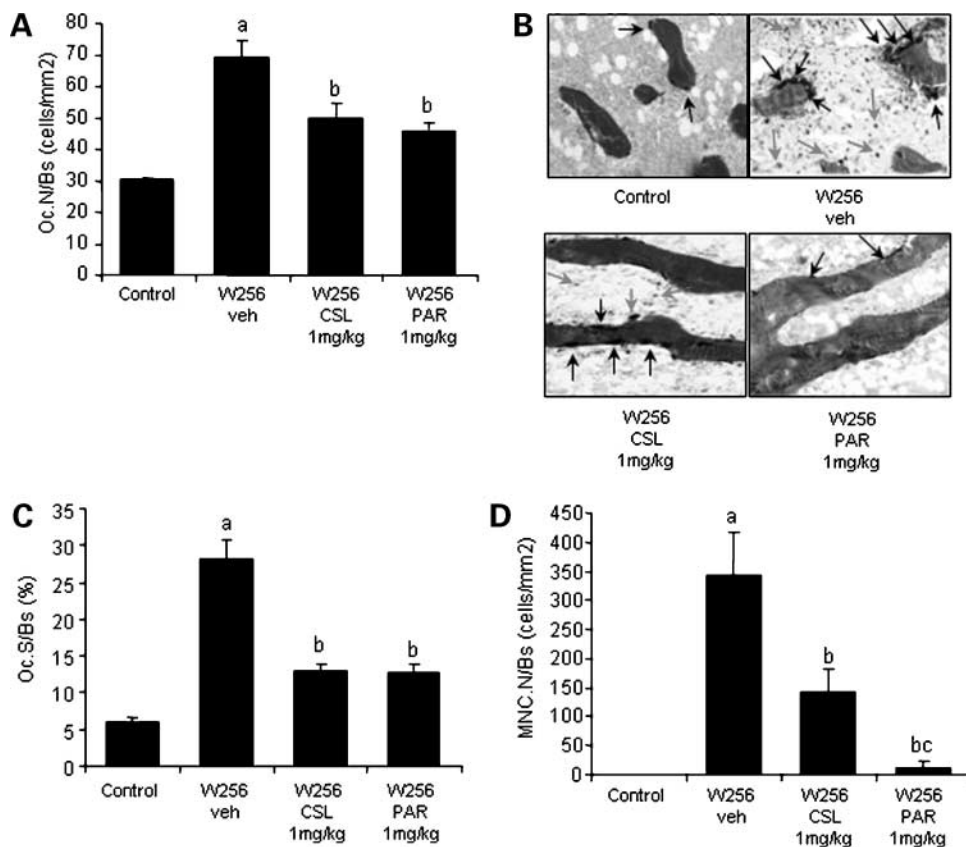


**Figure 6.** The IKK inhibitors celastrol (CSL) and parthenolide (PAR) inhibits the increase in osteoclast number and bone resorption following injection of W256 cells *in vivo*. Male Wistar rats at age of 16 wk received intracardiac injection of W256 tumor cells ( $10^7$  cells) followed by i.p. injection of either vehicle ( $n = 12$ ), celastrol (1 mg/kg/d;  $n = 12$ ), or parthenolide (1 mg/kg/d;  $n = 12$ ). Animals were sacrificed 10 d after injection and the limbs were embedded and processed for bone histomorphometry. **A**, the number of TRAcP-positive osteoclasts per bone surface area (Oc.N/BS). **B**, microphotograph of histologic stained sections showing TRAcP-positive mononucleated cells and multinucleated osteoclasts. *Black arrowheads*, multinucleated TRAcP-positive osteoclasts; *red arrowhead*, mononucleated TRAcP-positive cells. **C**, active resorption per bone surface area. **D**, the number of TRAcP-positive mononucleated cells per bone surface area (MNC.N/BS). *a*,  $P < 0.05$  from vehicle; *b*,  $P < 0.05$  from W256-injected group; *c*,  $P < 0.05$  from CSL-treated group.

intracardiac injections of W256 cells *in vivo*, thereby leading to higher bone volume and a more preserved architecture. Celastrol and parthenolide also reduced osteoclast numbers and inhibited bone resorption *in vivo*, consistent with the inhibitory effect on osteoclast formation and survival that was observed *in vitro* (12). Previous studies have shown that the IKK inhibitors used here can inhibit tumor growth directly in other animal models (18, 25, 27, 28). Although we observed a reduction in size of osteolytic lesions in this study, this might have been due to the inhibitory effects on osteoclast activity rather than an effect on tumor growth.

In this regard, previous studies with bisphosphonates have shown that both nitrogen and nonnitrogen-containing bisphosphonates are also effective at inhibiting osteolytic lesions in the Swiss Walker 256 model, whereas these agents have not been shown to have a systemic antitumor effect (39–42). In view of the fact that IKK inhibitors have a direct inhibitory effect on tumor growth in some tumor models, it would be of great interest in future studies to directly compare the effects of IKK inhibitors and bisphosphonates on the development of osteolytic lesions and systemic tumor growth in this model.

Although celastrol was more effective than parthenolide at suppressing W256 proliferation and migration and inducing apoptosis *in vitro*, both compounds had similar effects on the development of osteolytic metastases *in vivo*. This shows that pharmacologic inhibition of NF- $\kappa$ B at the level

of either TAK1 or IKK is equally effective at preventing osteolysis and bone loss *in vivo*. In conclusion, the results reported here show that pharmacologic inhibitors of the IKK complex suppress the growth and migration of W256 cells *in vitro* and prevent the development of bone metastases induced by injection of these cells *in vivo*. Although the work presented here indicates that IKK inhibitors could represent promising new agents for the treatment of metastatic bone disease, our studies were restricted to the W256 model and further studies will be required to determine if these agents are effective in preventing the development and progression of metastases in other disease models.

### Disclosure of Potential Conflicts of Interest

A.I. Idris: Bone Biology Fellowship from European Calcified Tissue Society. The other authors disclosed no potential conflicts of interest.

### References

- Mundy GR. Metastasis to bone: causes, consequences and therapeutic opportunities. *Nat Rev Cancer* 2002;2:584–93.
- Michaelson D, Talcott J, Smith M. Prostate cancer: metastatic. *Clin Evid* 2002;804–11.
- Raubenheimer EJ, Noffke CE. Pathogenesis of bone metastasis: a review. *J Oral Pathol Med* 2006;35:129–35.
- Guise TA. Molecular mechanisms of osteolytic bone metastases. *Cancer* 2000;88:2892–8.
- Hirbe A, Morgan EA, Uluckan O, Weilbaecher K. Skeletal complications of breast cancer therapies. *Clin Cancer Res* 2006;12:6309–14s.

6. Clement JF, Meloche S, Servant MJ. The IKK-related kinases: from innate immunity to oncogenesis. *Cell Res* 2008.
7. Karin M. The beginning of the end: I $\kappa$ B kinase (IKK) and NF- $\kappa$ B activation. *J Biol Chem* 1999;274:27339–42.
8. Gohda J, Akiyama T, Koga T, Takayanagi H, Tanaka S, Inoue J. RANK-mediated amplification of TRAF6 signaling leads to NFATc1 induction during osteoclastogenesis. *EMBO J* 2005;24:790–9.
9. Li J, Sarosi I, Yan XQ, et al. RANK is the intrinsic hematopoietic cell surface receptor that controls osteoclastogenesis and regulation of bone mass and calcium metabolism. *Proceedings of the National Academy of Sciences of the United States of America* 2000;97:1566–71.
10. Chaisson ML, Branstetter DG, Derry JM, et al. Osteoclast differentiation is impaired in the absence of inhibitor of  $\kappa$  B kinase  $\alpha$ . *J Biol Chem* 2004;279:54841–8.
11. Ruocco MG, Maeda S, Park JM, et al. I $\kappa$ B kinase (IKK) $\beta$ , but not IKK $\alpha$ , is a critical mediator of osteoclast survival and is required for inflammation-induced bone loss. *J Exp Med* 2005;201:1677–87.
12. Idris AI, Simic P, Krishnan M, Vukicevic S, Ralston S. Small molecule inhibitors of IKK-dependent signalling inhibit osteoclast formation *in vitro* and ovariectomy-induced bone loss *in vivo*. *Calcified Tissue International* 2008;82.
13. Gasparian AV, Yao YJ, Kowalczyk D, et al. The role of IKK in constitutive activation of NF- $\kappa$ B transcription factor in prostate carcinoma cells. *J Cell Sci* 2002;115:141–51.
14. Park BK, Zhang H, Zeng Q, et al. NF- $\kappa$ B in breast cancer cells promotes osteolytic bone metastasis by inducing osteoclastogenesis via GM-CSF. *Nat Med* 2007;13:62–9.
15. Jourdan M, Moreaux J, Vos JD, et al. Targeting NF- $\kappa$ B pathway with an IKK2 inhibitor induces inhibition of multiple myeloma cell growth. *Br J Haematol* 2007;138:160–8.
16. Luo JL, Tan W, Ricono JM, et al. Nuclear cytokine-activated IKK $\alpha$  controls prostate cancer metastasis by repressing Maspin. *Nature* 2007;446:690–4.
17. Lee DF, Kuo HP, Chen CT, et al. IKK  $\beta$  suppression of TSC1 links inflammation and tumor angiogenesis via the mTOR pathway. *Cell* 2007;130:440–55.
18. Kishida Y, Yoshikawa H, Myoui A. Parthenolide, a natural inhibitor of nuclear factor- $\kappa$ B, inhibits lung colonization of murine osteosarcoma cells. *Clin Cancer Res* 2007;13:59–67.
19. Guzman ML, Rossi RM, Neelakantan S, et al. An orally bioavailable parthenolide analog selectively eradicates acute myelogenous leukemia stem and progenitor cells. *Blood* 2007;110:4427–35.
20. Blouin S, Basle MF, Chappard D. Rat models of bone metastases. *Clin Exp Metastasis* 2005;22:605–14.
21. Blouin S, Basle MF, Chappard D. Interactions between microenvironment and cancer cells in two animal models of bone metastasis. *Br J Cancer* 2008;98:809–15.
22. Idris AI, Sophocleous A, Landao-Bassonga E, van't Hof RJ, Ralston SH. Regulation of bone mass, osteoclast function, and ovariectomy-induced bone loss by the type 2 cannabinoid receptor. *Endocrinology* 2008;149:5619–26.
23. Serrels A, Macpherson IR, Evans TR, et al. Identification of potential biomarkers for measuring inhibition of Src kinase activity in colon cancer cells following treatment with dasatinib. *Mol Cancer Ther* 2006;5:3014–22.
24. Idris AI, Ralston SH, van't Hof RJ. The nitrosylated flurbiprofen derivative HCT1026 inhibits cytokine-induced signalling through a novel mechanism of action. *Eur J Pharmacol* 2008;602:215–22.
25. Yang H, Chen D, Cui QC, Yuan X, Dou QP. Celastrol, a triterpene extracted from the Chinese "Thunder of God Vine," is a potent proteasome inhibitor and suppresses human prostate cancer growth in nude mice. *Cancer Res* 2006;66:4758–65.
26. Yip KH, Zheng MH, Feng HT, Steer JH, Joyce DA, Xu J. Sesquiterpene lactone parthenolide blocks lipopolysaccharide-induced osteolysis through the suppression of NF- $\kappa$ B activity. *J Bone Miner Res* 2004;19:1905–16.
27. Oka D, Nishimura K, Shiba M, et al. Sesquiterpene lactone parthenolide suppresses tumor growth in a xenograft model of renal cell carcinoma by inhibiting the activation of NF- $\kappa$ B. *Int J Cancer* 2007;120:2576–81.
28. Huang Y, Zhou Y, Fan Y, Zhou D. Celastrol inhibits the growth of human glioma xenografts in nude mice through suppressing VEGFR expression. *Cancer Lett* 2008;264:101–6.
29. Libouban H, Blouin S, Moreau MF, Basle MF, Audran M, Chappard D. Effects of risedronate in a rat model of osteopenia due to orchidectomy and disuse: densitometric, histomorphometric and microtomographic studies. *Micron* 2008;39:998–1007.
30. Libouban H, Moreau MF, Legrand E, Basle MF, Audran M, Chappard D. Comparison insight dual X-ray absorptiometry (DXA), histomorphometry, ash weight, and morphometric indices for bone evaluation in an animal model (the orchidectomized rat) of male osteoporosis. *Calcif Tissue Int* 2001;68:31–7.
31. Chappard D, Alexandre C, Riffat G. Histochemical identification of osteoclasts. Review of current methods and reappraisal of a simple procedure for routine diagnosis on undecalcified human iliac bone biopsies. *Basic Appl Histochem* 1983;27:75–85.
32. Sethi G, Ahn KS, Pandey MK, Aggarwal BB. Celastrol, a novel triterpene, potentiates TNF-induced apoptosis and suppresses invasion of tumor cells by inhibiting NF- $\kappa$ B-regulated gene products and TAK1-mediated NF- $\kappa$ B activation. *Blood* 2007;109:2727–35.
33. Hehner SP, Hofmann TG, Droge W, Schmitz ML. The antiinflammatory sesquiterpene lactone parthenolide inhibits NF- $\kappa$ B by targeting the I $\kappa$ B kinase complex. *J Immunol* 1999;163:5617–23.
34. Kobori M, Yang Z, Gong D, et al. Wedelolactone suppresses LPS-induced caspase-11 expression by directly inhibiting the IKK complex. *Cell Death Differ* 2004;11:123–30.
35. Burke JR, Pattoli MA, Gregor KR, et al. BMS-345541 is a highly selective inhibitor of I $\kappa$ B kinase that binds at an allosteric site of the enzyme and blocks NF- $\kappa$ B-dependent transcription in mice. *J Biol Chem* 2003;278:1450–6.
36. Li X, Massa PE, Hanidu A, et al. IKK $\alpha$ , IKK $\beta$ , and NEMO/IKK $\gamma$  are each required for the NF- $\kappa$ B-mediated inflammatory response program. *J Biol Chem* 2002;277:45129–40.
37. Yemelyanov A, Gasparian A, Lindholm P, et al. Effects of IKK inhibitor PS1145 on NF- $\kappa$ B function, proliferation, apoptosis and invasion activity in prostate carcinoma cells. *Oncogene* 2006;25:387–98.
38. MacMaster JF, Dambach DM, Lee DB, et al. An inhibitor of I $\kappa$ B kinase, BMS-345541, blocks endothelial cell adhesion molecule expression and reduces the severity of dextran sulfate sodium-induced colitis in mice. *Inflamm Res* 2003;52:508–11.
39. Krempien B, Wingen F, Eichmann T, Muller M, Schmahl D. Protective effects of a prophylactic treatment with the bisphosphonate 3-amino-1-hydroxypropane-1,1-bisphosphonic acid on the development of tumor osteopathies in the rat: experimental studies with the Walker carcinoma 256. *Oncology* 1988;45:41–6.
40. Krempien B, Manegold C. Prophylactic treatment of skeletal metastases, tumor-induced osteolysis, and hypercalcemia in rats with the bisphosphonate Cl2MBP. *Cancer* 1993;72:91–8.
41. Kurth AA, Muller R. The effect of an osteolytic tumor on the three-dimensional trabecular bone morphology in an animal model. *Skeletal Radiol* 2001;30:94–8.
42. Bassani D, Sabatini M, Scanziani E, et al. Bone invasion by Walker 256 carcinoma, line A in young and adult rats: effects of etidronate. *Oncology* 1990;47:160–5.

# Molecular Cancer Therapeutics

## Pharmacologic inhibitors of I $\kappa$ B kinase suppress growth and migration of mammary carcinosarcoma cells *in vitro* and prevent osteolytic bone metastasis *in vivo*

Aymen I. Idris, H el ene Libouban, Herv e Nyangoga, et al.

*Mol Cancer Ther* 2009;8:2339-2347. Published OnlineFirst August 11, 2009.

<b>Updated version</b>	Access the most recent version of this article at: doi: <a href="https://doi.org/10.1158/1535-7163.MCT-09-0133">10.1158/1535-7163.MCT-09-0133</a>
<b>Supplementary Material</b>	Access the most recent supplemental material at: <a href="http://mct.aacrjournals.org/content/suppl/2009/08/19/1535-7163.MCT-09-0133.DC1">http://mct.aacrjournals.org/content/suppl/2009/08/19/1535-7163.MCT-09-0133.DC1</a>

<b>Cited articles</b>	This article cites 39 articles, 14 of which you can access for free at: <a href="http://mct.aacrjournals.org/content/8/8/2339.full#ref-list-1">http://mct.aacrjournals.org/content/8/8/2339.full#ref-list-1</a>
<b>Citing articles</b>	This article has been cited by 8 HighWire-hosted articles. Access the articles at: <a href="http://mct.aacrjournals.org/content/8/8/2339.full#related-urls">http://mct.aacrjournals.org/content/8/8/2339.full#related-urls</a>

<b>E-mail alerts</b>	<a href="#">Sign up to receive free email-alerts</a> related to this article or journal.
<b>Reprints and Subscriptions</b>	To order reprints of this article or to subscribe to the journal, contact the AACR Publications Department at <a href="mailto:pubs@aacr.org">pubs@aacr.org</a> .
<b>Permissions</b>	To request permission to re-use all or part of this article, use this link <a href="http://mct.aacrjournals.org/content/8/8/2339">http://mct.aacrjournals.org/content/8/8/2339</a> . Click on "Request Permissions" which will take you to the Copyright Clearance Center's (CCC) Rightslink site.